Available online at www.sciencedirect.com
ScienceDirect
Journal of Magnetism and Magnetic Materials 318 (2007) 65–73
Journal of magnetism and magnetic materials
www.elsevier.com/locate/jmmm

Magnetism and transport of $CuCr_2Se_4$ thin films

J.S. Bettinger[a,*], R.V. Chopdekar[a,b], M. Liberati[c,d], J.R. Neulinger[e], M. Chshiev[f], Y. Takamura[a], L.M.B. Alldredge[a,b], E. Arenholz[d], Y.U. Idzerda[c], A.M. Stacy[e], W.H. Butler[f,g], Y. Suzuki[a]

[a]*Department of Materials Science and Engineering, UC Berkeley, Berkeley, CA 94720, USA*
[b]*School of Applied Physics, Cornell University, Ithaca, NY 14853, USA*
[c]*Department of Physics, Montana State University, Bozeman, MT 59717, USA*
[d]*Advanced Light Source, Lawrence Berkeley National Laboratory, Berkeley, CA 94720, USA*
[e]*Department of Chemistry, UC Berkeley, Berkeley, CA 94720, USA*
[f]*MINT Center, University of Alabama, Tuscaloosa, AL 35487, USA*
[g]*Department of Physics and Astronomy, University of Alabama, Tuscaloosa, AL 35487, USA*

Received 12 April 2007
Available online 25 April 2007

Abstract

We report on the successful synthesis, magnetism and transport of highly spin-polarized chalcogenide thin films of $CuCr_2Se_4$, which are promising candidates for spin-based electronic applications. We also present electronic structure calculations for $CuCr_2Se_4$ that, together with magnetic and transport data, imply that the stoichiometric compound is a metallic ferromagnet with a relatively low density of hole-like carriers at the Fermi energy. These calculations also predict that a deficiency of Se will deplete the minority density of states at the Fermi energy perhaps leading to a half-metal. We have successfully grown thin films of $CuCr_2Se_4$ by pulsed laser deposition on isostructural $MgAl_2O_4$ substrates followed by an anneal in a Se-rich environment. X-ray diffraction confirms the structure of $CuCr_2Se_4$ on $MgAl_2O_4$ substrates as well as a secondary phase of Cr_2Se_3. X-ray absorption spectroscopy indicates that the chemical structure at the surface of the films is similar to that of bulk $CuCr_2Se_4$ single crystals. Magnetization measurements indicate that these films saturate with a magnetic moment close to $5\,\mu_B$/f.u. and a Curie temperature (T_c) above 400 K. X-ray magnetic circular dichroism measurements show that magnetic order persists to the surface of the film. Resistivity and Hall effect measurements are consistent with p-type ferromagnetic metallic behavior and with the electronic structure calculations.
© 2007 Elsevier B.V. All rights reserved.

Keywords: Chalcogenide spinel thin films; Half-Metallic; Magnetic characterization; Electronic structure calculations

1. Introduction

Recently, there has been an enormous amount of research on the development of highly spin-polarized materials in light of their potential incorporation into spin-based electronic applications. However, fundamental questions remain concerning these highly spin-polarized materials and the nature of magnetism at surfaces and interfaces. Many of the studies on these materials have focused on binary and ternary oxides, including CrO_2, Fe_3O_4, $La_{0.7}Sr_{0.3}MnO_3$, and $SrFeMoO_6$ [1]. They have been successfully synthesized in thin film form and incorporated into prototypical spin-based devices.

While complex oxide materials have been well studied to this end, complex chalcogenides have not been explored for magnetic devices. Of particular interest is the family of chalcogenide spinels, AB_2X_4, where X is one of S, Se, or Te. In contrast to the oxide spinels, one may hope that the decrease in the ionic character of the bonds in the chalcogenides may lead to transport properties more similar to ordinary metals and semiconductors. The bulk properties of most chalcogenide spinels were examined in the 1960s. They exhibit a wide range of electronic and magnetic behavior [2–7]. Within the family of chalcogenide spinels, the basic structural parameters, such as the S–S or

*Corresponding author.
E-mail address: joannabettinger@berkeley.edu (J.S. Bettinger).

0304-8853/$ - see front matter © 2007 Elsevier B.V. All rights reserved.
doi:10.1016/j.jmmm.2007.04.024

Se–Se distances, as well as thermal properties such as thermal expansion are very similar for most members of the family, so epitaxial growth of thin isostructural multilayer structures is generally possible. Therefore, one can imagine synthesizing and fabricating an all-chalcogenide spinel multilayer magnetic device. In addition, these materials have recently been the object of renewed study as high magnetoresistance materials [8].

Of the many known chalcogenide spinel materials, $CuCr_2Se_4$ is a promising candidate for magnetic devices. Although this ferromagnetic metallic material that has been synthesized in bulk form since the 1960s [5], it has been proven difficult to grow as either a single crystal or a thin film. Most single crystals of this material have actually been halogen doped of the form $CuCr_2Se_{4-y}X_y$ (X = Cl, Br) and grown using chemical vapor transport with a halogen gas as a the transport agent [9]. Prior work on $CuCr_2Se_4$ thin films has been met with limited success [10–12]. Bulk forms of $CuCr_2Se_4$ have magnetization near $5\,\mu_B$/f.u. at low temperatures and have a relatively high Curie temperature (T_C) of 444 K [13]. Previously published data indicate that the crystal structure is a normal spinel [3,6,14], made of an FCC lattice of Se with Cu cations in 1/8 of the tetrahedral sites and Cr cations in 1/2 of the octahedral sites. More recent bulk work [13] indicates that the structure has a trigonal distortion while still being analogous to spinel, with edge-sharing octahedral Cr and corner sharing tetrahedral Cu. Bulk studies indicate that deviations from stoichiometry through Br-substitutions of the Se can give rise to poorer metallic conductivity and even semiconducting behavior [15].

2. Electronic structure calculations

The calculated electronic structure of $CuCr_2Se_4$ is shown in Figs. 1–3. The calculations were performed using the generalized gradient approximation (GGA) within density functional theory (DFT). The Vienna ab initio simulation program [16–21] implementation of DFT using projector augmented waves was employed for the calculations. The calculations shown here are based on a fully relaxed structure ($a = 10.395$ Å, $u = 0.00767$), but differed only slightly from those based on the high symmetry spinel structure and reported structural parameters [14] ($a = 10.334$ Å, $u = 0.00739$). Here, u represents the deviation of Se positions from the ideal FCC positions and is expressed in terms of fractions of the primitive vectors of the unit cell. The spin–orbit interaction was not included in the calculations and possible orbital contributions to the magnetization were neglected.

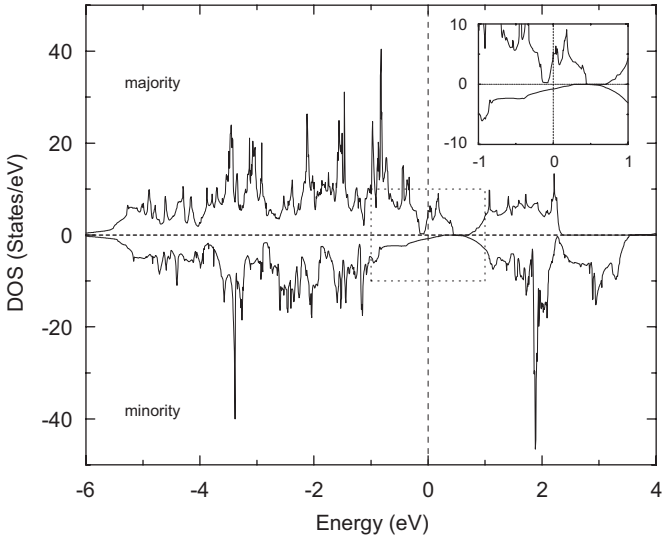

Fig. 1. Calculated density of electronic states for stoichiometric $CuCr_2Se_4$. Inset shows zoomed area around the origin.

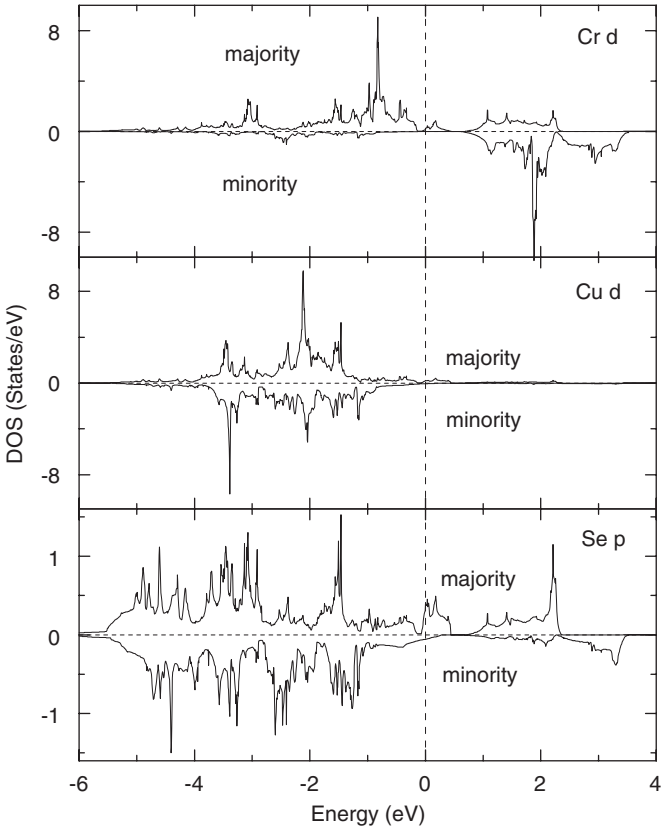

Fig. 2. Site and angular-momentum decomposed density of electronic states (Cr-d, Cu-d and Se-p) for $CuCr_2Se_4$.

Fig. 1 shows the total density of states, while Fig. 2 shows the density of states decomposed by site and angular momentum component. The Fermi level is indicated by a dashed line at 0 eV. The Se-p states are spread over a range of approximately 9 eV due to their hybridization with the Cr and Cu-d states. The Cr majority-d states hybridize with the Se-p states and spread from approximately 4 eV below the Fermi level to 2 eV above it. The Cr minority d-states are almost all above the Fermi-energy. The Se-p states are largely but not completely filled. The Cu-d states also hybridize strongly with the Se-p states, but lie somewhat higher on average than the Cr-d states. The Cu-d states are largely filled except for a few unfilled majority states. The

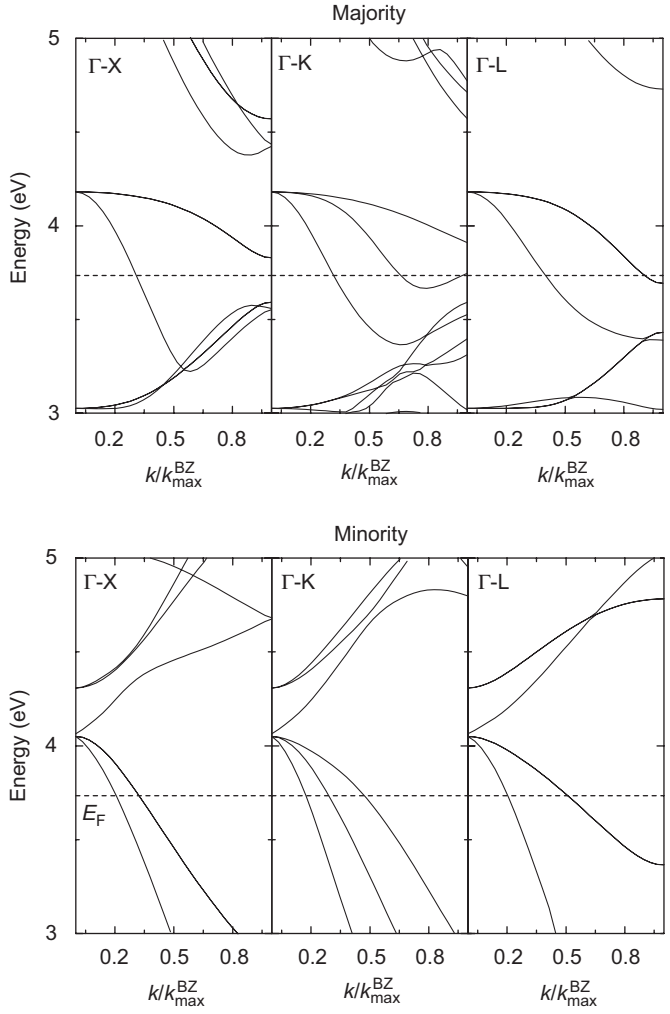

Fig. 3. Majority and minority energy bands near Fermi Energy (dashed line) along Γ–X, Γ–K and Γ–L directions.

magnetic moment lies mainly on the Cr atoms that have a moment of nearly $3\,\mu_B$/ion and are aligned ferromagnetically. The Cr moments are partially compensated by small moments of opposite sign on the Cu and Se atoms so that the total calculated moment is slightly greater than $5\,\mu_B$/f.u. ($5.12\,\mu_B$ or $338\,\text{emu/cm}^3$). It should be noted that this picture is similar to that deduced from neutron diffraction studies in Ref. [3] and from XMCD in Ref. [22].

We also performed LDA + U calculations (not shown) in which a Coulomb U of 5 eV was applied to the *d*-states of the Cu and Cr ions. Interestingly, while the total moment per formula unit increased to $5.61\,\mu_B$, the electronic structure did not change qualitatively from the GGA result. We expect correlation effects to be less important in the chalcogenides than the oxides because of the more extended nature of the ligand wave functions. For $CuCr_2Se_4$, the fact that the system is basically ferromagnetic with a very delocalized anti-ferromagnetic component (spread over the Se and Cu ions) rather than a ferrimagnetic system like most magnetic spinels, probably helps to delocalize the electrons and reduce the correlation effects that cannot be treated by the mean-field DFT–GGA approach. Our calculated DOS is similar to that calculated by Ramesha and Seshadri [23] using the LMTO method, but differs in two important aspects; their calculated magnetization is slightly higher ($5.2\,\mu_B$/f.u.) and their DOS does not show the gap in the minority DOS just above the Fermi energy.

The unfilled energy bands for both the majority and minority spin channels near the Fermi energy indicate that $CuCr_2Se_4$ is predicted to be metallic. The Fermi surface (Fig. 3) is relatively simple for the minority channel, which has three closed hole surfaces centered at the Γ-point. These three surfaces have relatively high dispersion as evidenced by the low and smooth density of states in the minority channel at the Fermi energy. Based on the calculated integrated DOS, we estimate that these three surfaces contain 0.065 holes/f.u. The smallest hole surface has a Fermi velocity of 5.5×10^5 m/s and an effective mass of $0.26m_e$ in the Γ-X direction. In this direction, the larger hole surfaces have a Fermi velocity of approximately 3.5×10^5 m/s and a mass of $0.65m_e$. We emphasize that the conduction electrons in this material differ qualitatively from the massive, low velocity electrons commonly encountered in transition metal oxides. Our calculated electronic structure in the vicinity of the Fermi energy is similar to that obtained by Ogata et al. [24] using the DV–Xα method. However, relativistic calculations [25] do not show the smallest minority hole surface because of a splitting that leaves the Γ point just above the Fermi energy doubly rather than triply degenerate.

The majority bands that cross the Fermi energy consist of a single highly dispersive band that forms a closed hole surface surrounding the Γ-point, and two additional, less dispersive bands that are degenerate along Γ–X and Γ–L. These two bands give the structure in the majority DOS that extends from just below the Fermi surface to a narrow gap in the majority DOS that begins approximately 0.2 eV above E_F. We estimate that the closed hole surface contains approximately 0.02 electrons/f.u. The electrical conductivity will depend not only on the number and velocities of the carriers but also on the scattering mechanisms that will depend on the temperature and on the concentration and types of defects. However, based on the Fermi surface alone, we would expect the current to be carried primarily by down-spin holes, thus making it a candidate for highly spin-polarized electrodes for magnetic tunnel junctions. The reason for this behavior is that more minority holes exist than majority holes (not counting the less dispersive bands) and the much higher density of states for majority than for minority holes is expected to increase the scattering rate for majority holes. An additional reason that we expect higher conductance from the minority bands is the absence of localized Cr-d states near the Fermi energy for the minority channel. The minority states near the Fermi energy seem to be quite delocalized, having contributions from all of the ions in the cell. Our picture of delocalized electrons at the Fermi energy seems to be

consistent with the measured resistivity [15], which is reported to be as low as 25 μΩ cm at low temperature, rising to approximately 300 μΩ cm at room temperature. Thus, $CuCr_2Se_4$ is a surprisingly good metal for a transition metal-based material with such a large unit cell.

An estimate of the carrier density based on the estimated volumes of the closed hole surfaces yields $4.1 \times 10^{20}\,cm^{-3}$ for the minority hole surfaces and $1.4 \times 10^{20}\,cm^{-3}$ for the majority closed hole surface. In addition, there are two majority open surfaces for which the designation hole or electron is ambiguous but which are likely to have larger regions with negative curvature (holes) than positive curvature. We have not attempted a rigorous calculation of the low-field Hall constant, which would require an average over the Fermi surface of the mean curvature weighted by the square of the electron velocity [26–28]. The experimental value of the Hall carrier density, n_H, obtained by the extrapolation of measurements on $CuCr_2Se_{4-x}Br_x$ to $x = 0$ [15], is consistent with hole conduction, but this value is an order of magnitude greater than our estimate of the carrier density based on the closed surfaces only. However, it should be emphasized that the Hall carrier density, $n_H = -1/(R_H ec)$ is only equal to the number of carriers for spherical Fermi surfaces.

3. $CuCr_2Se_4$ thin films

In the context of the calculated electronic structure, we present our study on the successful growth of crystalline magnetic thin films of $CuCr_2Se_4$ via a two-step process, first using pulsed laser deposition (PLD) to grow stoichiometric films, and then performing an anneal in a Se-rich environment to promote crystallization of the correct phase of $CuCr_2Se_4$. X-ray diffraction, as well as magnetic and electronic transport characterization, indicates that as-grown films are a combination of $CuCrSe_2$ and ferrimagnetic $Cr_{3-\delta}Se_4$. Following the Se-rich anneal, we can successfully synthesize metallic ferromagnetic $CuCr_2Se_4$ films. Soft X-ray absorption spectroscopy (XAS) indicates that the chemical structure at the surface of the films is similar to that of bulk $CuCr_2Se_4$. Bulk magnetic measurements indicate that these films saturate with a magnetic moment close to $5\,\mu_B$/f.u. and have a T_c above 400 K. X-ray magnetic circular dichroism (XMCD) measurements in electron yield mode, which probe about 5–10 nm into the sample, reveal strong circular dichroism in the post-annealed films, thus suggesting that the magnetic properties of the $CuCr_2Se_4$ persist to the surface and would thus be suitable for spin-based devices. Resistivity and Hall effect measurements are consistent with p-type ferromagnetic metallic behavior.

3.1. Thin film synthesis

We have synthesized these chalcogenide films by PLD followed by a post-deposition annealing step in a vacuum-sealed quartz tube with a Se source. For PLD, sintered ceramic targets of $CuCr_2Se_4$ were pressed from hand-ground $CuCr_{2.003}Se_{4.089}$ powder. The powder was prepared by mixing the elements in a vacuum-sealed quartz tube and heating to 800 °C for 7 days. This powder was then pressed into a target with a 0.5-inch inner diameter stainless steel die at room temperature to a pressure of 2500 lb with a hydraulic laboratory press. The pellet was then sintered for 22 h at 1150 °C in an evacuated quartz tube. We have determined that optimal thin film growth occurs in vacuum (base pressure of 1×10^{-6} Torr) at 600–650 °C on an isostructural (1 0 0) $MgAl_2O_4$ substrate. The KrF excimer laser (248 nm) was operated at 3 Hz and a fluence of 3–4.5 J/cm^2. Post-deposition annealing *ex situ* in vacuum-sealed quartz tubes with Se for 48 h at 475 °C promotes the growth of the spinel $CuCr_2Se_4$. This two-step process has enabled not only successful growth and characterization of $CuCr_2Se_4$, but also the investigation of other selenides that have not previously been studied in thin film form.

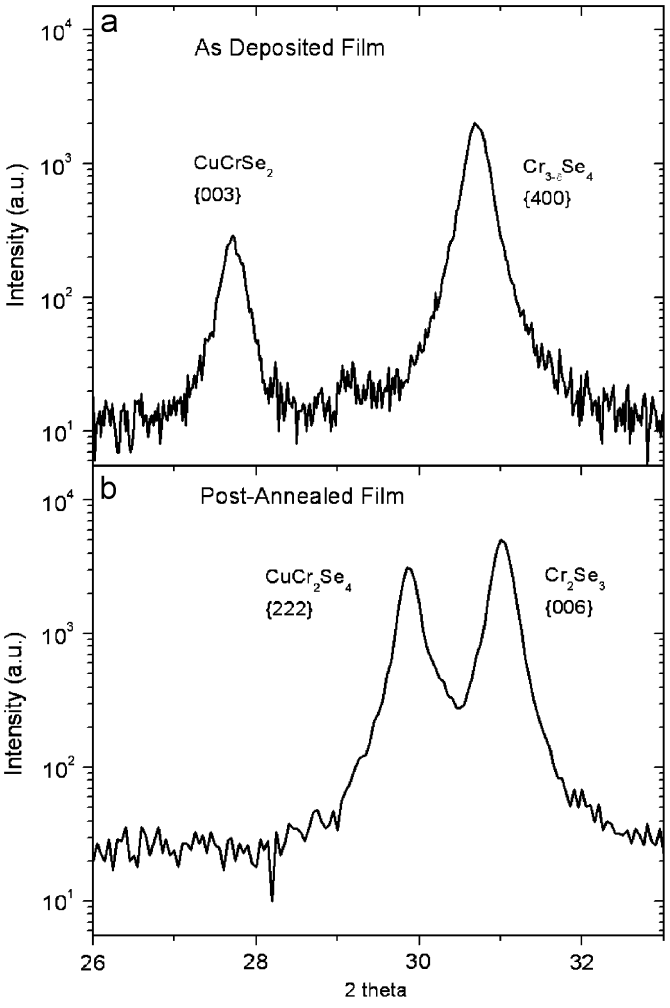

Fig. 4. X-ray diffraction pattern of (a) as deposited films of $CuCrSe_2$ and $Cr_{2.8}Se_4$ and (b) post-annealed films of the chalcogenide spinel $CuCr_2Se_4$ and Cr_2Se_3.

3.2. Structure

The structure of our films has been characterized through X-ray diffraction. In as-deposited films (Fig. 4a), we see reflections at 2θ values of 27.72° and 30.68°, corresponding to the $CuCrSe_2$ {0 0 6} and $Cr_{2.8}Se_4$ {4 0 0} planes. We also see higher order reflections at 2θ values of 57.12° and 63.80°, corresponding to the $CuCrSe_2$ {0 0 12} and $Cr_{2.8}Se_4$ {8 0 0} planes. Both crystal structures are similar to the spinel $CuCr_2Se_4$. $CuCrSe_2$ is made of an FCC lattice of Se with Cr in $\frac{1}{2}$ of the octahedral voids making $CrSe_2$ sandwiches, and Cu in $\frac{1}{2}$ of the tetrahedral voids between these sandwiches [29,30]. $Cr_{3-\delta}Se_4$ is an off-stoichiometric version of Cr_3Se_4 [31] which has a NiAs-like structure. In Cr_3Se_4, the Se anions make an HCP lattice with Cr in $\frac{3}{4}$ of the octahedral voids. $Cr_{3-\delta}Se_4$ is missing some of the Cr cations in the stoichiometric structure. After the Se anneal (Fig. 4b), we observe the reflections corresponding to the $CuCr_2Se_4$ {1 1 1} lattice planes. Additional reflections in the diffraction pattern are most likely attributed to Cr_2Se_3, an anti-ferromagnetic material with a Néel temperature (T_N) of 45 K [32]. From Rutherford backscattering spectrometry, we routinely find Cu deficiency in our films. This finding is consistent with the synthesis of Cr_2Se_3 along with $CuCr_2Se_4$ in the post-annealed films.

3.3. Magnetization

Through our two-step process, we have grown two different magnetic chalcogenides, $CuCr_2Se_4$ and $Cr_{3-\delta}Se_4$. $CuCr_2Se_4$ is predicted to be a highly spin-polarized spinel that has a T_c of 444 K. The magnetic moment comes from the occupation of the majority Cr d-states as described above. $Cr_{3-\delta}Se_4$ is an off-stoichiometric form of Cr_3Se_4. By changing the Cr content, it is possible to obtain an antiferromagnet or a ferrimagnet [31]. $Cr_{3+\delta}Se_4$ ($0 \leqslant \delta \leqslant 0.2$) is an antiferromagnet with T_N of 88 K for $\delta = 0$ and a decreasing T_N for increasing Cr content. $Cr_{3-\delta}Se_4$ ($0 < \delta \leqslant 0.2$), such as $Cr_{2.8}Se_4$ or $Cr_{2.9}Se_4$, is a ferrimagnet with a T_c of 88 K. The magnetism for $\delta = 0.2$ was suggested to be approximately $2\,\mu_B$/f.u. while the magnetism for the antiferromagnetic state of $\delta = 0$ must be $0\,\mu_B$.

A Quantum Design superconducting quantum interference device (SQUID) magnetometer was used to measure the magnetization as a function of applied field for as-grown and post-annealed films (Fig. 5a) with the applied magnetic field in the plane of the film. The magnetic properties of the as-grown films are dominated by ferrimagnetic $Cr_{2.8}Se_4$ while $CuCrSe_2$ only contributes a weak paramagnetic signal. The as-grown films saturate at 84 emu/cm^3, and magnetization versus temperature measurements indicate a magnetic transition around 70 K which is depressed from the bulk value of 88 K. Post-annealed films show saturation magnetization values of 293 emu/cm^3, or 4.4 μ_B/f.u., comparable with bulk values of approximately 5 μ_B/f.u. for $CuCr_2Se_4$. It is important to note that the presence of a Cr_2Se_3 phase in post-annealed films will artificially decrease the experimental magnetization values from a pure $CuCr_2Se_4$ phase. However, there is an additional effect of an increase in magnetization due to a Se-deficiency in the films, which will be discussed later. After Se annealing (Fig. 5b), magnetization versus temperature measurements show a Brillouin-like dependence with a magnetic transition above 400 K (the temperature limit of the SQUID magnetometer). The T_c is estimated to be approximately 405–410 K from the temperature dependence of magnetization slightly below 400 K.

We have also probed the chemical and magnetic properties within 5–10 nm of the surface of the post-annealed films by XAS and XMCD. These measurements were performed at a temperature of 14 K using total electron yield detection in 30° grazing X-ray incidence at the Lawrence Berkeley National Laboratory Advanced Light Source beamline 4.0.2. For the XMCD measurement, an external field of 0.53 T was applied. XAS (Fig. 6a) indicates that the chemical composition at the surface of post-annealed films is similar to that of the bulk [22]. XMCD spectra of Cr indicate that magnetic order persists

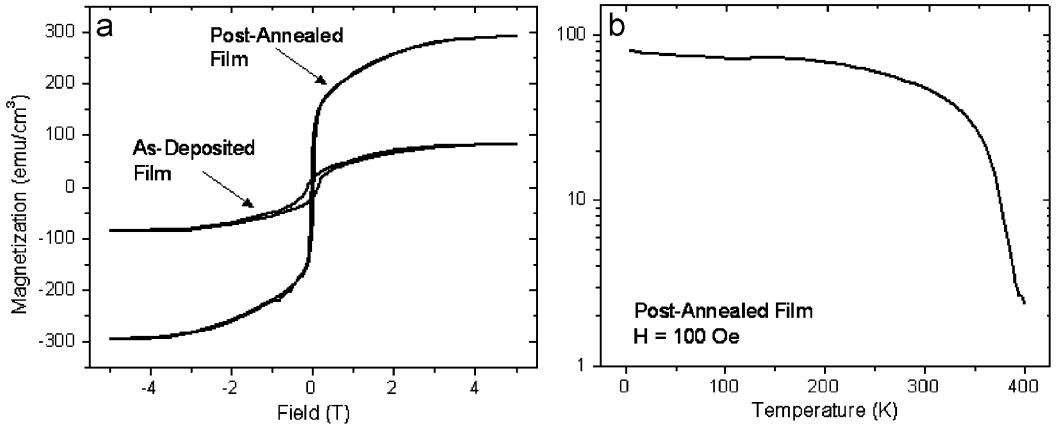

Fig. 5. (a) Magnetization vs. field measurements for as-deposited films containing $Cr_{2.8}Se_4$ measured at 10 K and post-annealed films of $CuCr_2Se_4$ measured at 5 K; (b) Magnetization vs. temperature of the post-annealed film of $CuCr_2Se_4$.

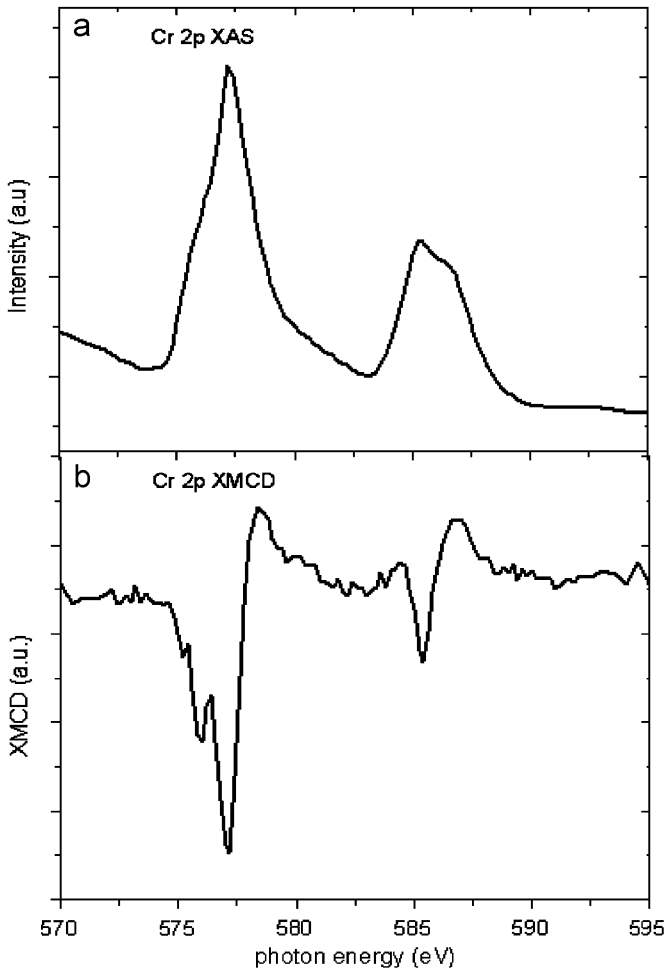

Fig. 6. Measurements taken at 14 K and a 30° grazing incidence of (a) XAS of $CuCr_2Se_4$ showing a characteristic lineshape for Cr in an octahedral environment; (b) Cr XMCD of $CuCr_2Se_4$ showing the persistence of magnetism to the surface of the film. XMCD measurement used an external field of 0.53 T.

to the surface of the post-annealed films (Fig. 6b). Moreover, the XMCD lineshape is characteristic of Cr in an octahedral environment and compares well to bulk data [22].

3.4. Transport

The electronic transport properties of these films have been studied by measuring resistivity as a function of temperature at different fields applied out of the plane of the film surface. Both as-grown and post-annealed films exhibit metallic behavior (Fig. 7). As-grown films exhibit a kink in the metallic behavior that is coincident with the Curie temperature of $Cr_{2.8}Se_4$. Such a kink is characteristic of ferromagnets in the vicinity of T_c and corresponds to the disappearance of scattering due to long-range spin disorder below T_c. The resistivity values of approximately $1.8\times10^{-3}\,\Omega$ cm at 320 K and $1.4\times10^{-3}\,\Omega$ cm at 10 K are those of a poor metal and all of these observations are consistent with bulk studies of $Cr_{2.8}Se_4$ [31]. The transport

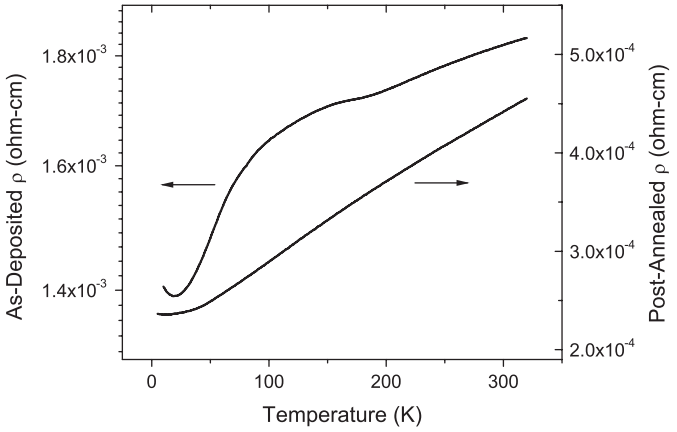

Fig. 7. Resistivity versus temperature transport data demonstrating the poor metallic behavior of as-grown $Cr_{2.8}Se_4$ films and metallic behavior of $CuCr_2Se_4$ films.

properties of as-grown films are nearly identical to bulk $Cr_{2.8}Se_4$ measurements, suggesting that the transport is dominated by $Cr_{2.8}Se_4$ and not $CuCrSe_2$. In contrast, the post-annealed samples exhibit metallic behavior similar to bulk $CuCr_2Se_4$ with resistivity values ranging from $5\times10^{-4}\,\Omega$ cm at 400 K to $2\times10^{-4}\,\Omega$ cm at 10 K [15]. We also observe a flattening out of the resistivity curve at low temperatures. We fit the low-temperature resistivity data to the Bloch–Gruneissen formula, $A+BT^n$, and found the coefficient n to be approximately 2.7, implying that the low temperature scattering is largely electron–electron and electron–magnon scattering. The relatively high resistivity together with a metal-like increase in the resistivity with temperature suggests a low carrier density.

We have also studied both the anomalous and ordinary Hall Effect as a function of temperature in post-annealed thin films in order to probe the carrier concentration of $CuCr_2Se_4$ as well as the effects of impurity scattering. Fig. 8a shows both the anomalous and ordinary contributions to the Hall resistance at 5 and 300 K. The ordinary contribution indicates that this material is a p-type metal with an average carrier concentration of about $3\times10^{20}\,\mathrm{cm}^{-3}$ over the entire temperature range. The anomalous Hall effect (AHE) is examined by subtracting out the linear background representing the contribution of the ordinary Hall effect (Fig. 8b), and there is a crossover in the sign of the AHE resistivity at 287 K. Bulk crystal data [15] also indicates that $CuCr_2Se_4$ is a p-type metal but with a much higher carrier concentration. We acknowledge that the ordinary Hall effect is not a good measure of the actual carrier concentration for materials with complicated electronic structure. However, the differences in carrier concentration between bulk single crystals and films of $CuCr_2Se_4$ need to be addressed. We attribute these differences to the effects of impurities due to the presence of Cr_2Se_3 and a Se deficiency. A reduction in carrier concentration is also found in single crystals of $CuCr_2Se_{4-x}Br_x$ where Br is introduced as a dopant on

the Se site [15]. The anomalous contribution nearly saturates at temperatures below 100 K with a small decrease in magnitude at very low temperature, and decreases in magnitude as a function of increasing temperature above 100 K; the anomalous Hall signal eventually switches sign at higher temperatures as seen in Fig. 8b. We measured anomalous Hall coefficients, R_s, as a function of temperature (Fig. 8c) and found that the temperature dependence and magnitude of R_s is consistent with recent data of bulk $CuCr_2Se_{4-x}Br_x$ for small values of x. Therefore, impurity scattering in our films must be taken into consideration due to the presence of non-magnetic Cr_2Se_3. We believe this to be the first study of Se-deficient $CuCr_2Se_4$ of any form including thin films, crystals, and bulk powder.

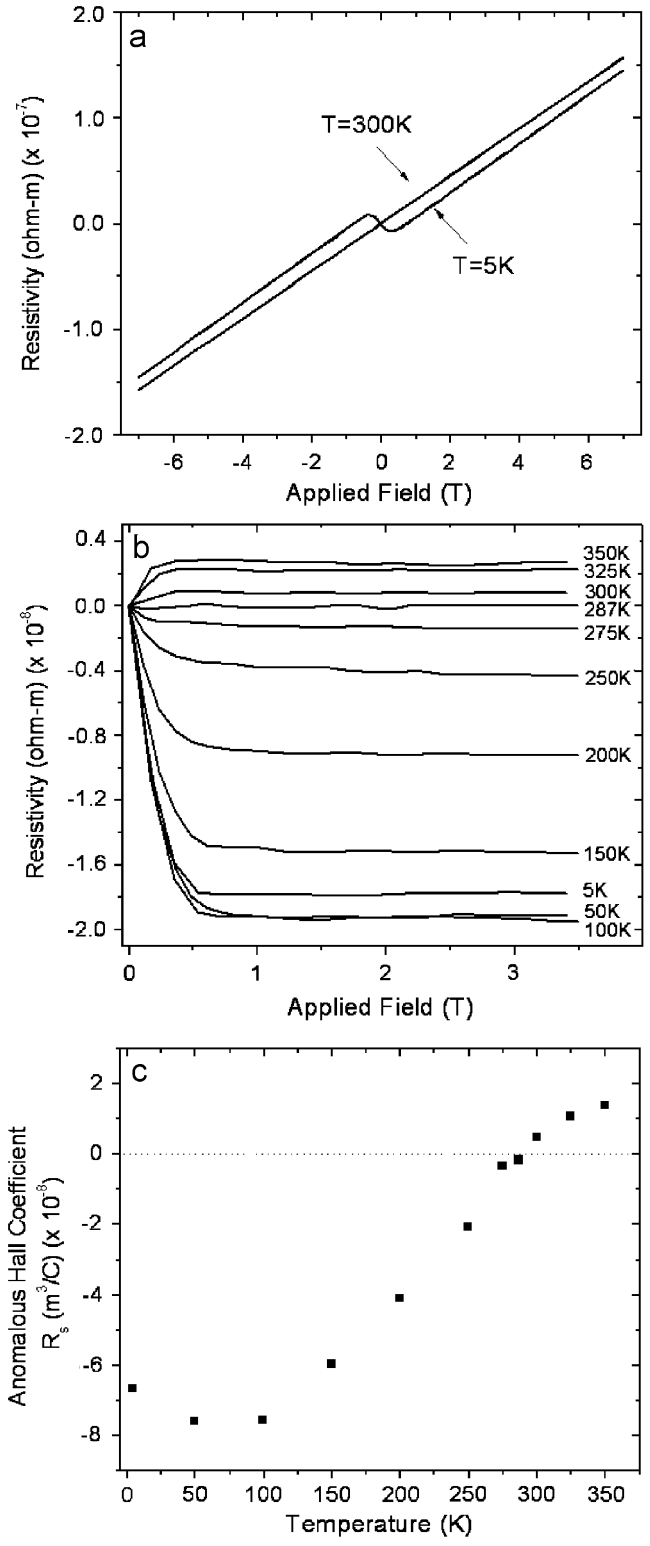

Fig. 8. (a) Total Hall effect, containing both the ordinary and anomalous contributions to the Hall effect at 5 and 300 K of $CuCr_2Se_4$ films; (b) anomalous contribution to the Hall effect from 5 to 350 K of $CuCr_2Se_4$ films; (c) anomalous Hall coefficient, R_s, from 5 to 350 K in $CuCr_2Se_4$ films.

4. Se vacancies in $CuCr_2Se_4$

In order to model the effect of Se vacancies in $CuCr_2Se_4$, we calculated the electronic structure of $Cu_2Cr_4Se_7$. One Se atom was removed from the 14 atom basis of the FCC spinel cell and the resulting structure was relaxed. The structural relaxation resulted in a cell with a small trigonal distortion and a 3.6% increase in volume. Just as in the stoichiometric spinel structure, each Se atom is surrounded by 1 Cu and 3 Cr ions. However, small changes exist in the nearest-neighbor distances that generate three slightly different Se environments. One of the Cu atoms retains four Se neighbors while the other has only three. One of the Cr atoms retains six neighboring Se atoms while the other three have only five.

The density of states is shown in Figs. 9 and 10 where the Fermi level is indicated by a dashed line at 0 eV. The most noticeable effect of the Se vacancy is that the Fermi energy falls in a gap for the minority implying that the substoichiometric material (at least in this ordered form) is a half-metal. The magnetic moment increases to 6 μ_B (382 emu/cm^3). Though our films have a second impurity

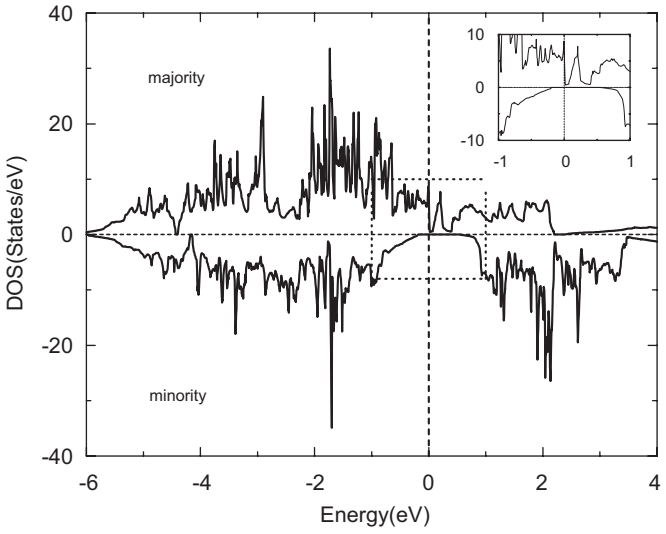

Fig. 9. Calculated density of electronic states for substoichiometric $CuCr_2Se_{3.5}$ with a Se vacancy. Inset shows zoomed area around the origin.

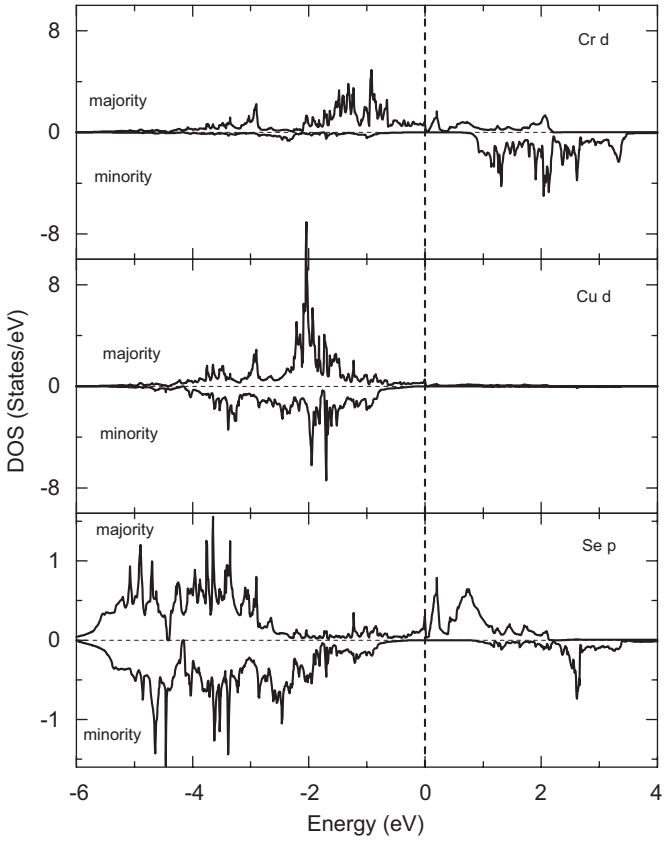

Fig. 10. Site and angular-momentum decomposed density of electronic states (Cr-d, Cu-d and Se-p) for substoichiometric $CuCr_2Se_{3.5}$.

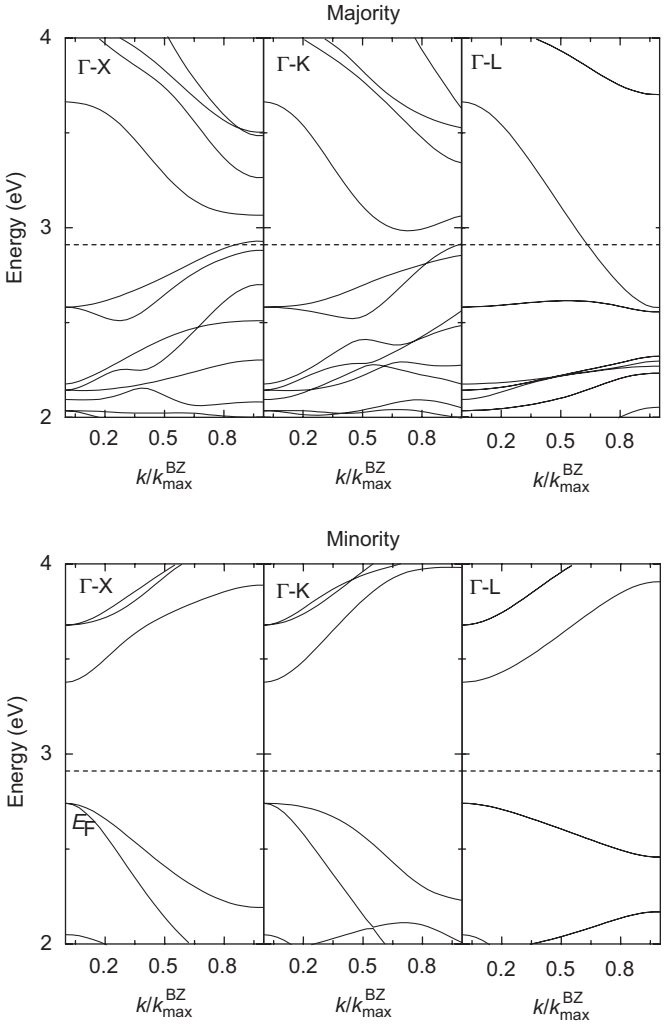

Fig. 11. Majority and minority energy bands near Fermi Energy (dashed line) along Γ–X, Γ–K and Γ–L directions for substoichiometric $CuCr_2Se_{3.5}$.

phase, their Se-deficiency helps to increase the saturation magnetization closer to the bulk value of the stoichiometric phase. Compared to the stoichiometric system, it appears that all of the ions (except for one Se) have lost minority spins (or gained majority spins).

The Cu-d states for the Cu atom adjacent to a Se vacancy rise by approximately 0.2 eV. There is a narrow peak in the majority just above the Fermi energy that arises from Cr-d states on Cr ions adjacent to the vacancy, and from Se-p states on Se ions that are adjacent to the 3 Cr, each of which lost a Se neighbor. For the minority channel, the vacancy causes the Se-p states to narrow slightly at the upper edge resulting in a gap at the Fermi energy.

The Fermi surface properties are strongly modified (Fig. 11). The three minority hole surfaces disappear, as does the closed majority hole surface, leaving only open majority surfaces at the Fermi energy. It is difficult to compare the calculations for the ordered Se-deficient material with the experimental measurements because the vacancies are presumably disordered and their concentration is not determined. However, the calculations do indicate that Se vacancies will likely decrease the density of hole-like carriers. This result is qualitatively consistent with our experimental result of $n_H = 3 \times 10^{20}\,cm^{-3}$ which is much lower than the reported bulk value of $7 \times 10^{21}\,cm^{-3}$.

5. Conclusions

In this work, we have demonstrated the successful synthesis of thin films of $CuCr_2Se_4$ that are theorized to be highly spin polarized. The structural, chemical, magnetic, and transport characterization confirm that we have been successful in $CuCr_2Se_4$ film growth, and have shed light on the magnetic and transport properties associated with this thin film. We have also confirmed that their magnetic properties persist to the surface. Electronic structure calculations indicate delocalized electrons at the Fermi energy and the possibility of half-metallic behavior for substoichiometric films, making these films promising candidates for future spin-based electronic devices.

Acknowledgments

The authors thank Kin Man Yu for RBS characterization and Jennifer E. Johnson for fruitful discussions. This work was funded by the NIRT program of the National

Science Foundation (#0303774). The Advanced Light Source is supported by the US Department of Energy, Basic Energy Sciences, under Contract no. DE-AC02-05CH11231. Work at UA was also supported by MRSEC Grant DMR0213985 and by the INSIC EHDR Program.

References

[1] J.M.D. Coey, C.L. Chien, MRS Bull. 28 (2003) 720.
[2] P.F. Bongers, C. Haas, A.M.J. Vanrun, G. Zanmarch, J. Appl. Phys. 40 (1969) 958.
[3] C. Colominas, Phys. Rev. 153 (1967) 558.
[4] J.B. Goodenough, Solid State Commun. 5 (1967) 577.
[5] F.K. Lotgering, Solid State Commun. 2 (1964) 55.
[6] M. Robbins, H.W. Lehmann, J.G. White, J. Phys. Chem. Solids 28 (1967) 897.
[7] R.J. Bouchard, P.A. Russo, A. Wold, Inorg. Chem. 4 (1965) 685.
[8] A.P. Ramirez, R.J. Cava, J. Krajewski, Nature 386 (1997) 156.
[9] K. Miyatani, K. Minematsu, Y. Wada, F. Okamoto, K. Kato, P.K. Baltzer, J. Phys. Chem. Solids 32 (1971) 1429.
[10] V.N. Berzhansky, N.A. Drokin, V.I. Ivanov, V.P. Kononov, I.S. Edelman, S.A. Havrichkov, V.K. Chernov, A.G. Shishkov, A.M. Pirogova, Thin Solid Films 190 (1990) 199.
[11] S. Yamanaka, S. Kobayash, S. Nakai, M. Naoe, Jpn. J. Appl. Phys. 10 (1971) 668.
[12] V.N. Berzhanskii, S.A. Gavrichkov, V.P. Kononov, S.V. Misyul, Inorg. Mater. 16 (1980) 561.
[13] J. R. Neulinger, J. E. Johnson, A. M. Stacy, unpublished.
[14] I. Okonskakozlowska, J. Kopyczok, H.D. Lutz, T. Stingl, Acta Crystallogr. C 49 (1993) 1448.
[15] W.L. Lee, S. Watauchi, V.L. Miller, R.J. Cava, N.P. Ong, Science 303 (2004) 1647.
[16] G. Kresse, J. Hafner, Phys. Rev. B 47 (1993) 558.
[17] G. Kresse, J. Hafner, Phys. Rev. B 49 (1994) 14251.
[18] G. Kresse, J. Furthmuller, Comput. Mater. Sci. 6 (1996) 15.
[19] G. Kresse, J. Furthmuller, Phys. Rev. B 54 (1996) 11169.
[20] P.E. Blochl, Phys. Rev. B 50 (1994) 17953.
[21] G. Kresse, D. Joubert, Phys. Rev. B 59 (1999) 1758.
[22] A. Kimura, J. Matsuno, J. Okabayashi, A. Fujimori, T. Shishidou, E. Kulatov, T. Kanomata, Phys. Rev. B 63 (2001) 224420.
[23] K. Ramesha, R. Seshadri, Solid State Sci. 6 (2004) 841.
[24] F. Ogata, T. Hamajima, T. Kambara, K. Ichiro, J. Phys. C 15 (1982) 3483.
[25] V.N. Antonov, V.P. Antropov, B.N. Harmon, A.N. Yaresko, A.Y. Perlov, Phys. Rev. B 59 (1999) 14552.
[26] W.H. Butler, Phys. Rev. B 29 (1984) 4224.
[27] M. Tsuji, J. Phys. Soc. Jpn. 13 (1958) 818.
[28] M. Tsuji, J. Phys. Soc. Jpn. 13 (1958) 979.
[29] F.M.R. Engelsman, G.A. Wiegers, F. Jellinek, B. Van Laar, J. Solid State Chem. 6 (1973) 574.
[30] P.F. Bongers, C.F. Van bruggen, J. Koopstra, W.P.F.A.M. Omloo, G.A. Wiegers, F. Jellinek, J. Phys. Chem. Solids 29 (1968) 977.
[31] A. Maurer, G. Collin, J. Solid State Chem. 34 (1980) 23.
[32] M. Yuzuri, J. Phys. Soc. Jpn. 35 (1973) 1252.